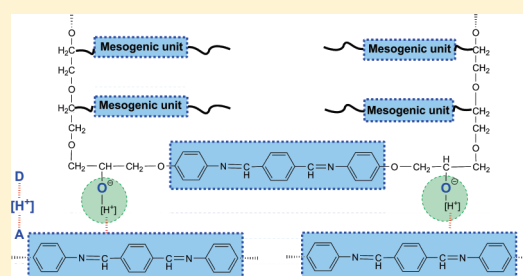


Structure–Property Relationship of Highly π -Conjugated Schiff-Base Moiety in Liquid Crystal Diepoxide Polymerization and Mesophases Stabilization

Huan Liu,^{†,‡} Zien Fu,^{†,‡} Kai Xu,^{*,†} Hualun Cai,^{†,‡} Xin Liu,^{†,‡} and Mingcai Chen[†][†]Key Laboratory of Polymer Material for Electronics, Guangzhou Institute of Chemistry, Chinese Academy of Sciences, P.O. Box 1122, Guangzhou 510650, People's Republic of China[‡]Graduate School of the Chinese Academy of Sciences, Beijing 100049, People's Republic of China**S** Supporting Information

ABSTRACT: A study of the structure–property relationship of the highly π -conjugated Schiff-base moiety in polymerization of a liquid crystal (LC) diepoxide oligomer (PBMBA) and mesophases stabilization has been investigated. We first proposed two exothermic peaks distinctly observed in nonisothermal polymerization curves for thermal copolymerization of PBMBA monomer with a diamine comonomer that corresponded to two different reactions, namely, an epoxy-amine polymerization and anionic polymerization. For PBMBA, note that an unexpected homopolymerization accompanying an appearance of enantiotropic mesophase transitions had taken place in the absence of any initiators, evidencing the possibility of an anionic mechanism yielding a homopolymer. A novel Schiff-base model compound (SBM) was synthesized and used to induce the polymerization of different types of epoxies. Based on the structure–property relationship, we considered a specific role of highly π -conjugated Schiff-base moieties in the anionic polymerization of PBMBA and hoped the mesophases could be stabilized using this mechanism, which may provide a key strategy for design of the polymer-dispersed liquid crystal (PDLC) materials via a chemical process.



INTRODUCTION

Owing to their superior electrical and mechanical properties, ease of processing, good adhesion to many substrates, and excellent chemical resistance, epoxy polymers have been widely used as structural, coating, and adhesive materials in many demanding application fields, such as automotive, aeronautics, electronics, and electrical engineering.^{1–4} Recently, epoxy-based polymers also contribute to the development of advanced functional materials, such as self-healing polymers,^{5,6} shape memory polymers,^{7,8} hybrid organic–inorganic polymers,^{9,10} and thermoresponsive inorganic/organic polymers.^{11,12} The important research in materials consisting of specific organic structure units (such as mesogenic group, π -conjugated moiety, etc.) embedded in an epoxy matrix have been developed.^{13,14} One way to prepare these organic–organic functional materials is to find the optimum interplay of weak and strong physical interactions (supramolecular chemistry) with covalent bonds (crosslinks). This implies the strategy not only of the chemistry, but also of the rheology and thermodynamics in the same process.

In the absence of a detailed understanding of the supramolecular interactions between the individual π -conjugated molecules, the introduction of π -conjugated systems in electronic devices and the dream to arrive at molecular electronics based on these systems have become one of the most challenging scientific

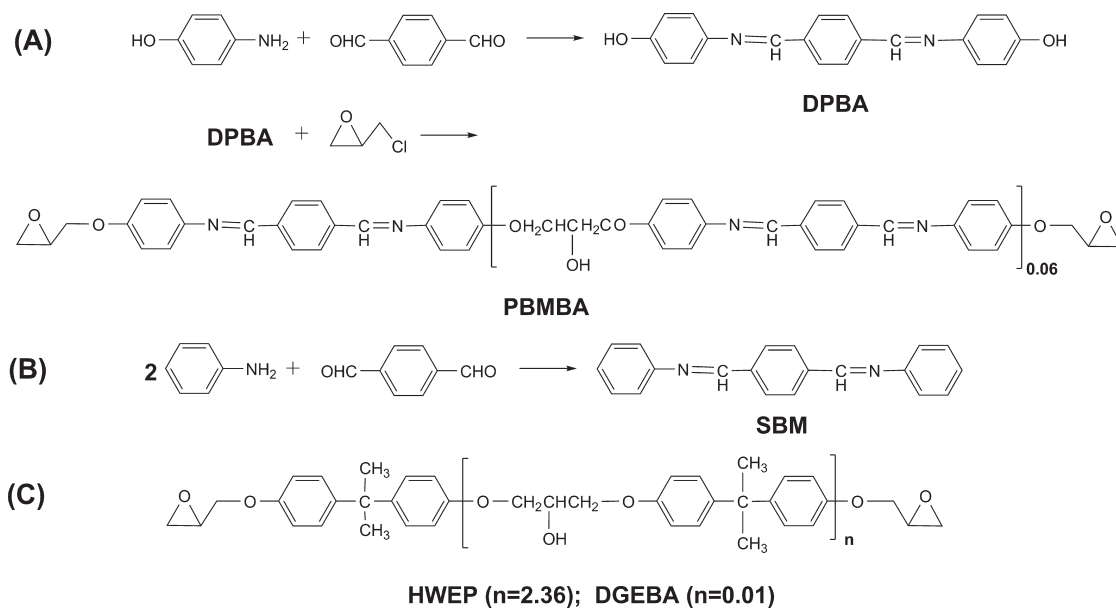
research areas. Intensive research has been dedicated to the ability of self-assembly of π -conjugated systems, which has mainly been approached from both a materials and a supramolecular chemistry point of view.^{15–18} Based on the ability of self-assembly of π -conjugated systems, π -conjugated polymer chains acting as rigid chains could function as mesogenic units for liquid crystal properties.^{19–21} However, ordered structures formed by LC mesophases have a well-known drawback, they are difficult to be stabilized, which limits their wide application. According to the theory of supramolecular chemistry, two important secondary interactions in mesophase formation and stabilization are π – π ²² and hydrogen bond interactions. Generally, π – π interactions often exist in π -conjugated systems and hydrogen bonds are formed when a donor (D) with an available acidic hydrogen atom is interacting with an acceptor (A) carrying available nonbonding electron lone pairs. In comparison with the π – π interactions, the hydrogen bonds, being highly selective and directional, are ideal secondary interactions to construct supramolecular architectures. Use of intermolecular hydrogen bonding, the controlled morphology of epoxy-based responsive polymers has been reported.^{23–27} Special interests have been

Received: March 31, 2011

Revised: May 9, 2011

Published: May 23, 2011

Scheme 1. Synthetic Routes of PBMBA (A) and SBM (B); Chemical Structure of Epoxy (C)



focused on the design of the epoxy-based responsive polymers with controlled dispersion of the low molar mass liquid crystals to find correlations between fast response to the external field, such as thermal gradient, electric, or magnetic fields, and the final morphology generated in these systems. Several representative low molar mass crystal structures are known for EBBA that was used to generate polymer-dispersed liquid crystals (PDLCs) by polymerization-induced phase separation (PIPS) in an epoxy matrix.^{28,29} This type of PDLC, consisting of well-dispersed and stabilized LC-rich domains in a polymer matrix, displays functional properties and is a material with a potential application in electrooptical devices.^{30–32}

In this work, the liquid crystal diepoxide oligomer (PBMBA), alternately having imine groups (C=N) and benzene rings in the main chain and being π -conjugated through rigid molecular scaffolds, was prepared in a manner similar to the method reported in ref 33. This polymer was investigated since early 1998 and was reported to show enantiotropic mesophase transitions;^{33–35} however, to our knowledge, the specific role of a highly π -conjugated Schiff-base moiety in the polymerization of PBMBA has not been investigated from the point of view of the structure–properties relationship. Meanwhile, whether these ordered structures appearing in the vicinity of the enantiotropic mesophase transitions temperature region of both the smectic and nematic phases could be stabilized by using this anionic homopolymerization of the one-component LC diepoxide that has not yet been reported. As one aim of this study, we are going to focus on its anionic polymerization mechanism of the LC diepoxide based on the structure–property relationship of a highly π -conjugated Schiff-base moiety in the polymerization of PBMBA. For the PBMBA/MDA copolymerization system, two exothermic peaks were distinctly observed in nonisothermal polymerization curves, and corresponding various enthalpies during the two polymerization stages could be derived, which is considered as two different reaction mechanisms: the epoxy-amine polymerization reaction and the anionic polymerization reaction. Note that the anionic initiation mechanism, being different from the one reported by others,^{34,35} was first proposed.

This type of anionic initiation mechanism could also be used to explain the occurrence of the unexpected homopolymerization accompanying with the appearance of enantiotropic mesophase transitions in the absence of any initiators for the nonisothermal polymerization curve of PBMBA. Likewise, we hoped that the highly π -conjugated Schiff-bases moiety could also initiate the polymerization of different types of epoxies. Accordingly, a Schiff-base model compound (SBM) was synthesized and used to induce the polymerization of epoxy. Owing to the simultaneity of the mesophase transitions and the homopolymerization, we wondered whether these mesophases could not be disrupted and could even be stabilized using this reaction. As a second aim of this study, differential scanning calorimetry (DSC), polarizing optical microscopy (POM), and wide-angle X-ray diffraction (WAXD) were used to explore the possibility of stabilization of mesophases via a chemical process. Once the LC ordered structures could be stabilized by the homopolymerization of the diepoxide, there can be no doubt for a new strategy for the design of the PDLC materials via a chemical process, which will be the focus of our further study.

EXPERIMENTAL SECTION

Materials. All reagents and solvents were purchased as reagent grade and were purified or dried by standard methods before use. The following reagents were purchased from Aladdin-reagent Co. Shanghai, China: terephthalaldehyde, *p*-aminophenol, aniline, and 4,4'-diaminodiphenylmethane (MDA). Analytical grade zinc chloride obtained from Shanghai Chemical Reagent, Ltd., China, was used as catalyst. Epichlorohydrin (ECH) was purchased from Lingfeng Chemical Reagent Co., Shanghai, China. The epoxies DGEBA (diglycidyl ether of bisphenol A) and HWEPE (high molecular weight diglycidyl ether of bisphenol A; see Scheme 1C) with an epoxy equivalent weight (EEW) of 185 g/eq and 502 g/eq were purchased from Shell Chemical Co. BAEP (bisphenol A diglycidyl ether) monomer was purchased from Alfa Aesar.

Physical Measurements. ^1H NMR spectrum was recorded on a Bruker AM-400S (400 MHz) spectrometer using TMS as internal standard and chloroform-*d* (at 7.26 ppm), DMSO-*d* (at 2.50 ppm), and acetone-*d* (at 2.05 ppm) as solvents. FT-IR spectrum was recorded with an Analect RFX-65A infrared spectrophotometer using KBr discs. EA was performed on a PE 2400 Series II CHNS/O Analyzer. Mass spectrum was determined on a VG-7070E spectrometer (EI, 70 eV).

Synthesis of PB MBA and SBM. The synthetic pathways of PB MBA and SBM are shown in Scheme 1. The procedures were carried out in a four-neck round-bottom flask equipped with a nitrogen inlet and stirrer under controlled temperature and pressure. Schiff-base-type diphenol (DPBA) was synthesized from terephthalaldehyde (20.0 g, 0.15 mol) and *p*-aminophenol (30.0 g, 0.3 mol) in a solvent mixture (dimethyl sulfoxide (DMSO) 150 mL, ethanol (EtOH) 300 mL), using zinc chloride (0.5 g) as the catalyst (see Scheme 1A). The reaction mixture was stirred at 85 °C for 4 h and then poured into 1000 mL of H_2O . A yellow solid was collected by filtration, recrystallized, and dried. The liquid crystal (LC) diepoxide oligomer (PB MBA) was synthesized from 0.1 mol of DPBA, 5 mol of ECH, and 20 mL of DMSO as a solvent using 22.0 g of a 40 wt % NaOH solution as the catalyst (see Scheme 1A). SBM was synthesized via the condensation of terephthalaldehyde with aniline in a similar way as described in the synthesis of DPBA (see Scheme 1B).

DPBA: Yield, 42.0 g, 90%. mp, 272–275 °C. ^1H NMR (DMSO-*d*) δ (ppm): 9.57 (1H, single, OH), 8.57 (1H, single, N=CH), 7.80 (2H, single, ArH), 7.24–7.26 (2H, multiplet, ArH), 6.80–6.82 (2H, multiplet, ArH). FT-IR (KBr cm^{-1}): 3384 (OH), 1619 (CN). MS: m/z 316 [M^+]. Elem. Anal. (%) Calcd for $\text{C}_{20}\text{H}_{16}\text{N}_2\text{O}_2$: C, 75.93; H, 5.10; N, 8.86; O, 10.11. Found: C, 75.77; H, 5.15; N, 8.81; O, 10.27.

PB MBA: mp: 194–203 °C. ^1H NMR (CDCl_3) δ (ppm): 8.51 (1H, single, N=CH), 7.97 (2H, single, ArH), 7.24–7.26 (2H, multiplet, ArH), 6.94–6.96 (2H, multiplet, ArH), 4.85 (1H, single, OH), 4.23–4.27 (2H, multiplet, CH_2), 3.95–4.00 (2H, multiplet, CH_2), 3.53–3.38 (1H, multiplet, CH), 2.90–2.91 (2H, multiplet, CH_2), 2.76–2.78 (2H, multiplet, CH_2). FT-IR (KBr cm^{-1}): 3384 (OH), 1610 (CN), 914 (epoxy ring). EEW: 225 g/eq.

SBM: Yield: 24.5 g, 86%. mp: 160–162 °C. ^1H NMR (acetone-*d*) δ (ppm): 8.68 (1H, single, N=CH), 8.10 (2H, single, ArH), 7.41–7.45 (2H, multiplet, ArH), 7.28–7.32 (2H, multiplet, ArH), 7.24–7.28 (1H, multiplet, ArH). FT-IR (KBr cm^{-1}): 1617 (CN). MS: m/z 284 [M^+]. Elem. Anal. (%) Calcd for $\text{C}_{20}\text{H}_{16}\text{N}_2$: C, 84.48; H, 5.67; N, 9.85. Found: C, 84.53; H, 5.65; N, 9.82.

DSC Experiment. Differential scanning calorimetry (DSC) was recorded with a Diamond/Pyris DSC analyzer under a nitrogen atmosphere. For the mixture of PB MBA/MDA, PB MBA was dissolved completely in chloroform, and then a stoichiometric amount of MDA was added. Afterward, the solvent was removed by rotary evaporator under reduced pressure. Three mixtures of SBM/BAEP, SBM/DGEBA, and SBM/HWEP with a 1:1 mol ratio of C=N and epoxy were prepared in the same way as mentioned above. The nonisothermal DSC copolymerization of PB MBA/MDA was recorded under nitrogen from 50 to 300 °C at heating rates of 5, 10, 15, 20 °C/min. For the homopolymerization of PB MBA, the same type of experiment has been carried by DSC from 50 to 320 °C. For the study of SBM, the mixtures of SBM/BAEP, SBM/DGEBA, and SBM/HWEP and the corresponding neat diepoxides were

heated from 50 to 300 °C at a heating rate of 10 °C/min under nitrogen.

Calculation of Activation Energy Value (E_a). E_a obtained with respect to the analysis of secondary reactions and the conversion of epoxy groups at the end of the DSC runs allowed the following assumptions in the further analysis of DSC data: (i) negligible influence of secondary reactions; (ii) 100% conversion of the limiting reactant; and (iii) heat of reaction constant and independent of conversion. The DSC data were correlated to the rate of conversion at constant temperature to some function of the concentration of reactants using the following equation:

$$\frac{d\alpha}{dt} = kf(\alpha) \quad (1)$$

where $(d\alpha)/(dt)$ is the rate of cure; α is the fractional conversion at any time t ; k , the Arrhenius rate constant, and $f(\alpha)$, a function form of α that depends on the reaction mechanism. For nonisothermal conditions, when the temperature varies with time with a constant heating rate, $\beta = dT/dt$, eq 1 is represented as follows:

$$\frac{d\alpha}{dT} = \frac{A}{\beta} \exp\left(-\frac{E_a}{RT}\right) f(\alpha) \quad (2)$$

where A is the pre-exponential factor, E_a is the activation energy, and R is the gas constant. The straightforward application of eqs 1 and 2 yields a single kinetic triplet for the overall process. This type of analysis does not allow for possible changes in the rate-limiting step. The derivative modes by Dole can be used to give E_a from the plot $\ln \beta_i$ against $T_{\alpha i}^{-1}$ (here i is the ordinal number of DSC runs performed at different heating rates, β_i).³⁶

UV–Vis Experiment. Ultraviolet and visible light (UV–vis) absorbance spectrum was measured using a Shimadzu UV-2550 spectrophotometer (Shimadzu Corporation, Kyoto, Japan). The measurements of the optical absorption were performed at room temperature, where a deuterium lamp is a source of ultraviolet (200–380 nm) and a tungsten lamps are used for visible (380–800 nm) and near-infrared (800–3300 nm) parts of light. The samples, PB MBA, MDA and mixture of PB MBA/MDA (1:1 mol ratio) were well soluble in the nonpolar chloroform (CHCl_3). The concentration of these solutions has been on the level 10^{-5} mol/L, suitable for the UV–vis optical investigations.

POM Experiment. Optical studies were conducted with a polarizing optical microscope (POM; Optiphot-Po1, Nikon) equipped with a hot stage attachment (Mettler FP52/FP5). The phase and crystalline morphology of different types of aggregation structures were observed under POM with a heating rate of 10 °C/min. For the stabilization of the smectic phase, PB MBA was heated from room temperature to 225 °C (a temperature of smectic–nematic transition) but soon dropped to 210 °C. Heated at this temperature for 30 and 120 min, respectively, the samples, namely, as S30 and S120, were obtained. For the stabilization of the nematic phase, PB MBA was heated from room temperature to 240 °C (a temperature of nematic–isotropic transition) but soon dropped to 210 °C. Heated at this temperature for 30 and 50 min, respectively, the samples, namely, as N30 and N50, were obtained. During the entire observation period, we found the fixed mesophases could be sustained 120 min for the smectic phase and 50 min for the nematic phase. The given temperature, 210 °C, was found to be

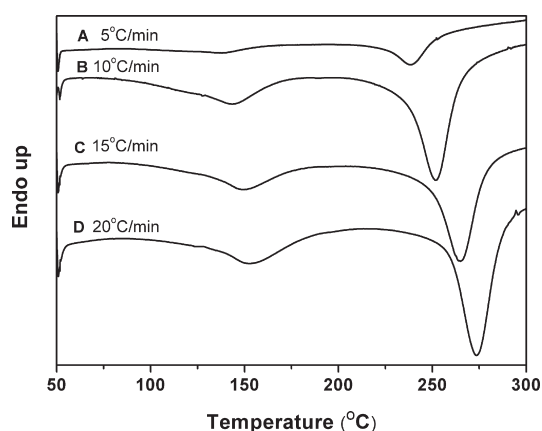


Figure 1. Nonisothermal DSC curves for the PBMBA/MDA copolymerization at various heating rates.

the most suitable temperature for the stabilization of the LC ordered structures.

FT-IR Experiment. The samples prepared for observing a shift of PBMBA CH=N absorption band using FT-IR spectra were obtained by DSC calcination at a heating rate of 10 °C/min under nitrogen. The two samples, obtained at 290 °C for PBMBA-1 and at 320 °C for PBMBA-2 were rapidly taken out from the DSC pool and quenched in liquid nitrogen.

WAXD Experiment. Wide angle X-ray diffraction (WAXD) scanning curves ranging from 0 to 60° were collected at room temperature with a Rigaku D/max-1200 X-ray diffractometer using copper filtered Cu K α radiation (40 KV, 30 mA). The samples, S30, S120, N30, and N50, with a glass slide as substrate, were used to perform WAXD measurements.

RESULTS AND DISCUSSION

PBMBA/MDA Copolymerization. Copolymerization Kinetics. The thermal copolymerization of PBMBA monomer with MDA comonomer was studied by DSC. The nonisothermal DSC polymerization curves at the various heating rates (see Figure 1) showed two exothermic peaks that were distinguished clearly from each other. For instance, the polymerization curve obtained at the heating rate of 10 °C/min exhibited one broad exothermic peak ranging from 70 to 190 °C and the other broad exothermic peak ranging from 200 to 300 °C. The peak temperature, T_p , and the polymerization enthalpy, ΔH , values for each exothermic peak obtained from Figure 1 are summarized in Table 1. As can be seen, T_p and the polymerization enthalpy values for stage 2 were considerably higher than those for stage 1. T_{p2} s appearing at the higher temperatures and corresponding ΔH s largely increased. The observed heat of PBMBA/MDA copolymerization for the stage 1 was calculated as 38 kJ/mol (based on a molecular weight of 450 g/mol obtained by titration), which was lower by almost 58 kJ/mol than that reported in the literature for the polymerization of epoxy/diamine, 98–99 kJ/mol.³⁷ This observation suggested 40% epoxy monomer conversion (α) during stage 1. Moreover, the observed heat for stage 2 was calculated as 95 kJ/mol. The resulting activation energies for each peak were, respectively, found to be $E_{a1} = 124.65$ kJ/mol for stage 1 and $E_{a2} = 82.27$ kJ/mol for stage 2.

The characteristic phenomena related to the appearance of two exothermic peaks and the corresponding and prodigiously different T_p , ΔH , and E_a values, occurring in the PBMBA/MDA

Table 1. Thermogravimetric Data for the Nonisothermal DSC at Various Heating Rates of the PBMBA/MDA Copolymerization

heating ratio (β ; °C/min)	T_{p1} (°C)	T_{p2} (°C)	ΔH_1 (J/g)	ΔH_2 (J/g)	E_{a1} (kJ/mol)	E_{a2} (kJ/mol)
5	137.96	238.64	-65.73	-179.72	124.65	82.27
10	143.45	252.21	-92.51	-234.88		
15	149.17	264.95	-84.19	-219.04		
20	152.90	273.57	-86.76	-199.30		

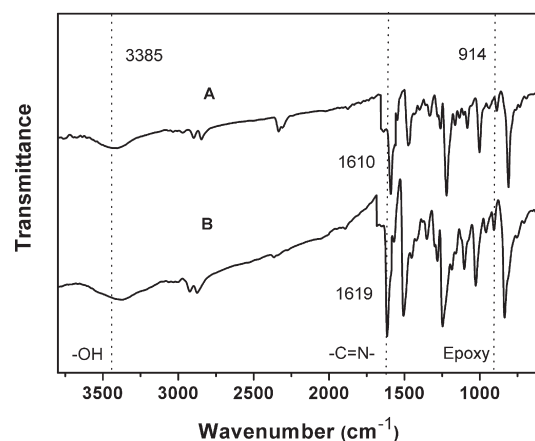


Figure 2. FT-IR spectra of PBMBA (A) and PBMBA/MDA (B).

copolymerization reaction, have attracted considerable attention. It is generally accepted that the epoxy-amine polymerization reaction includes three principle reactions: the reaction of the primary amine hydrogen with the epoxy group, the reaction of the secondary amine hydrogen with the epoxy group, and the reaction of the hydroxyl hydrogen with the epoxy group. These abnormalities in the PBMBA/MDA copolymerization reaction suggest that it did so through dissimilar mechanisms. For stage 1, the classical epoxy-amine polymerization reaction, nucleophilic addition on the epoxy ring proceeds with the preliminary activation of the epoxy ring by amines, takes place. In contrast to the results for E_a of the epoxy-amine polymerization reported by other researchers,^{38–41} the E_a value of PBMBA/MDA copolymerization for low conversion ($\alpha = 0–0.4$) is considerably high. This may be due to the specific role of highly π -conjugated Schiff-base in the copolymerization of PBMBA/MDA. Regarding stage 2, it can be noted that the onset polymerization of this stage starts after the end of stage 1. According to the literature,^{39,41,42} the reactions of stage 2 may become diffusion controlled at a higher conversion. However, due to the presence of the rigid rod-like mesogen, the increasing diffusion restriction hinders the mobility of the functional groups, which was further evidenced by higher T_p s for stage 2. The larger ΔH value implies that the reaction occurring in this stage can be attributed to the anionic polymerization reaction of the epoxy,³⁴ different from the epoxy-amine polymerization. The mechanism of the anionic polymerization being different from other authors' elucidation will be discussed further below.

FT-IR Spectrum and UV-Vis Absorbance Spectrum. The presence of the imine groups was confirmed, respectively, by FT-IR spectrum and UV-vis absorbance spectrum because the band characteristic of the C=N stretching deformations was

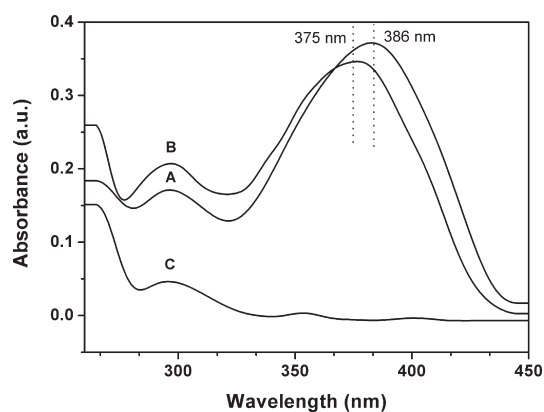


Figure 3. Chloroform solution UV–vis absorbance spectra of PB MBA (A), PB MBA/MDA (B), and MDA (C).

detected in the case of both PB MBA and PB MBA/MDA. In the FT-IR spectrum of PB MBA (see Figure 2), a strong absorption at 1610 cm^{-1} suggested the presence of the C=N structure, which shifted to a higher wavenumber in the case of PB MBA/MDA (1619 cm^{-1}). In addition to the C=N stretching band, a band at about 1590 cm^{-1} could be distinguished and ascribed to the C=C stretching deformations in the aromatic ring. The lower wavenumber of the imine group absorption indicates the better conjugation of π -electrons. The higher wavenumber value implies that the bond between carbon and nitrogen atoms in the imine group is shorter, which means that the π -electrons in the double bond are less involved in conjugation.

Figure 3 illustrates the UV–vis absorbance spectra, within the optical range from 260 to 450 nm, of PB MBA and PB MBA/MDA respectively in chloroform solution. The short-wave's border of UV spectra of solution was limited by a permeability of solvent, i.e. 240 nm for chloroform. Two absorbance bands at λ_1 (280–320 nm) and at λ_2 (320–440 nm) were distinctly present in the spectra of PB MBA and PB MBA/MDA, except that of MDA. PB MBA exhibited one well-defined absorption band in the range of 325–440 nm, being responsible for π – π^* transition in the imine group.^{43,44} The introduction of MDA to PB MBA in comparison with neat PB MBA led to a hypsochromic shift of the λ_{max} band in chloroform solution from 386 to 375 nm. The blue shift of the absorption maxima observed for the Schiff-base moiety described here is ascribed to the resonance effect of the protonic electron-withdrawing group.^{44,45} These results reveal that due to the presence of the highly π -conjugated imine structure acting as a proton acceptor and amino proton acting as a proton donor in chloroform solution, the assembly behavior of donor–proton–acceptor ($\text{D}\cdots[\text{H}^+]\cdots\text{A}$) shown in Figure 4 may be readily achieved in solution.⁴⁴ The protonation process of the Schiff-base moiety causes “break” of the conjugation system and diminishes the length of conjugated part of molecule, which leads to the hypsochromic transition of the long-wavelength absorption band.

Combination of evidence in the FT-IR spectrum and the UV–vis absorbance spectrum, the shift transitions of the characteristic peak for the C=N stretching deformations are consistent with the assembly behavior of $\text{D}\cdots[\text{H}^+]\cdots\text{A}$ between the Schiff-base moiety and the amino group.

Copolymerization Mechanism. The mechanism of the thermal copolymerization of PB MBA/MDA is postulated to attempt to elucidate our experimental observations that could not be explained simply by the classical epoxy-amine polymerization

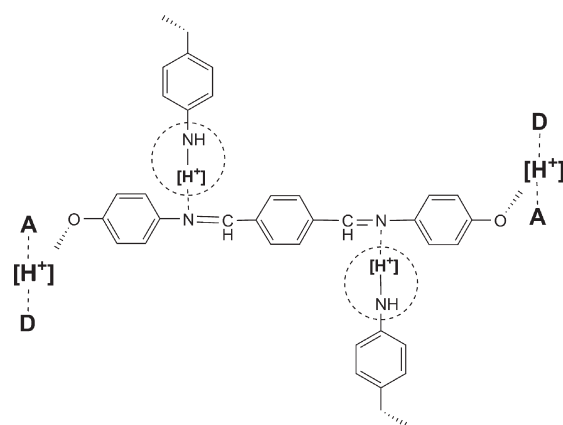


Figure 4. Proposed $\text{D}\cdots[\text{H}^+]\cdots\text{A}$ assembly model between the highly π -conjugated imine structure and the amine.

reaction. For stage 1, because the primary amines of MDA are involved in the protonation process of the Schiff-base moiety achieved in solution, the mobility of those is decreased. When the epoxy-amine copolymerization occurs, more energy is needed to achieve a deprotonation process that makes the primary amines be released, thus, resulting in the increase of the E_a values. When the reaction becomes the diffusion controlled at the higher conversion, the hydroxyl groups, initially present in the epoxy prepolymer and those generated during the epoxy-amine copolymerization, may move and are involved into the $\text{D}\cdots[\text{H}^+]\cdots\text{A}$ assembly. As shown in Figure 5, the $\text{D}\cdots[\text{H}^+]\cdots\text{A}$ assembly between the hydroxyl groups and the Schiff-base moiety leads to the formation of alkoxy anions. The formed key intermediate alkoxy anions can react with another hydroxyl groups that are not involved into the protonation process of the Schiff-base moiety through the ionic transition effect, which results in the formation of hydroxyl oxygen anions. This step can be considered to be the initiation process of the anionic polymerization (see Figure 6A). Based on this type of initiation mechanism, the hydroxyl oxygen anion can be regarded as initiation center that reacts with another epoxy ring, placing the actively site on another alkoxy anion. Thus, a kinetic chain causing branching and cross-linking is generated (see Figure 6B).

Rozenberg has acknowledged that the presence of a proton donor or electrophilic agent such as a hydroxyl group forming a complex between the hydroxyl group, the oxygen in the epoxy ring and the tertiary amine that is required by initiation of epoxy anionic polymerization by tertiary amines.⁴⁶ Many other researchers suppose that the initiation mechanism involves formation of a zwitter-ion by interaction between the tertiary amine and the H-bonded oxirane ring and that the subsequent propagation reaction occurs via the alkoxide.^{35,47–49} Whatever the true underlying initiation mechanism, they all focused their attention on the important role of tertiary amine that was beneficial to the formation of alkoxide or alkoxide anion, both of which could be the propagation species. However, it is necessary to point out no tertiary amines was used in our work. Accordingly, from the point of view of structure–properties relationship, it requires us to take into account what is the specific role of the highly conjugated Schiff-base moiety in polymerization of the epoxies.

PB MBA Homopolymerization. If the anionic polymerization was initiated by the protonation process of the Schiff-base moiety, this type of initiation mechanism should not only be suitable for the PB MBA homopolymerization, but also be

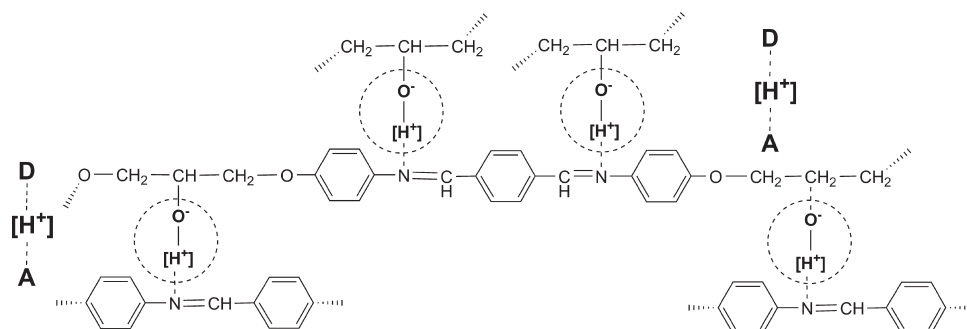


Figure 5. Proposed $D \cdots [H^+] \cdots A$ assembly model between the highly π -conjugated imine structure and the hydroxyl group.

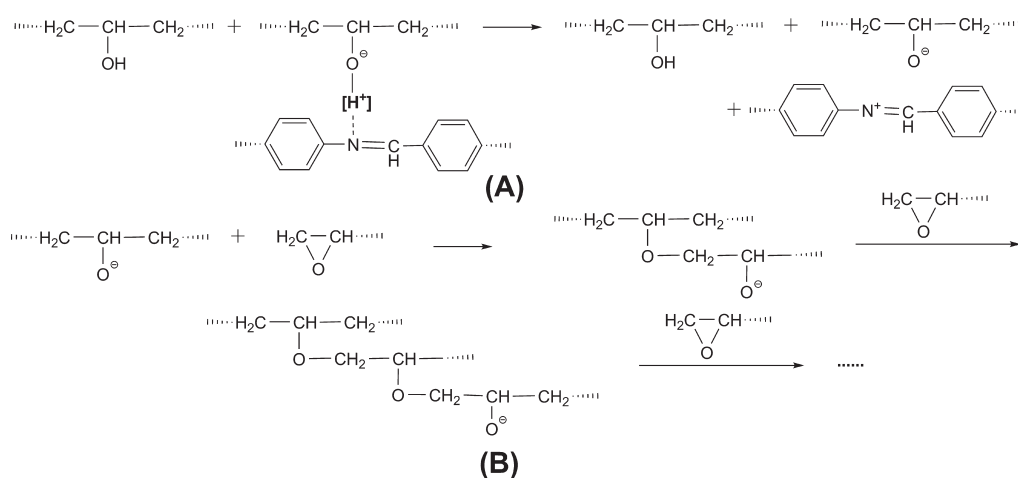


Figure 6. Proposed anionic polymerization for initiation (A) and propagation (B).

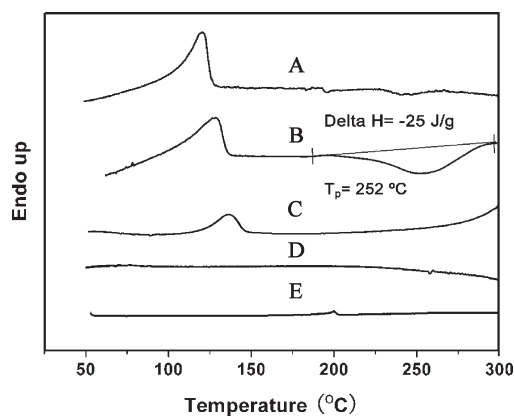


Figure 7. Nonisothermal DSC curves for SBM/DGEBA (A), SBM/HWEP (B), SBM/BAEP (C), DGEBA (D), and HWEP (E) at a heating rate of $10\text{ }^{\circ}\text{C}/\text{min}$.

suitable for SBM/epoxies system. Therefore, the specific role of the highly conjugated Schiff-base moiety in polymerization of the epoxies will be discussed in detail in the following chapter. The additional work on discovering the feasibility of the stabilization of the mesophases using the anionic homopolymerization also will be described below.

DSC and FT-IR Investigations. The DSC thermogram recorded for PBMBA (see Figure 8) showed three endothermic

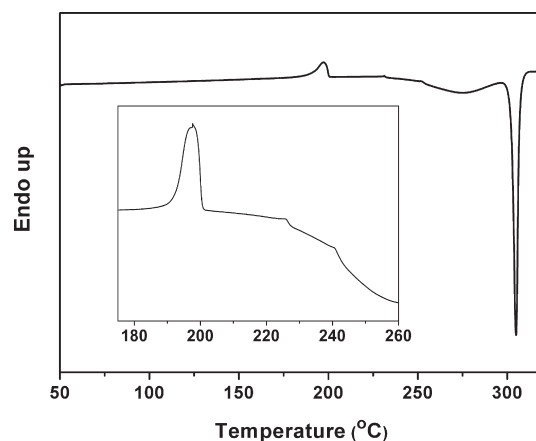


Figure 8. Nonisothermal DSC curves for the PBMBA homopolymerization at a heating rate of $10\text{ }^{\circ}\text{C}/\text{min}$.

peaks and two exothermic peaks. Table 2 shows T_p and ΔH values for each exothermic peak and each endothermic peak obtained from the dynamic DSC. The resulting activation energies for each peak were, respectively, found to be $E_{a1} = 93.90\text{ kJ/mol}$ for stage 1 and $E_{a2} = 120.73\text{ kJ/mol}$ for the stage 2. For the three endothermic peaks, the first one appearing in the broad range $180\text{--}207\text{ }^{\circ}\text{C}$, with a maximum peak value at $198\text{ }^{\circ}\text{C}$, was due to the monomer melting. The other two weak

Table 2. Thermogravimetric Data for the Nonisothermal DSC at the Various Heating Rates of the PBMB A Homopolymerization

heating ratio (β ; °C/min)	T_{p1} (°C)	T_{p2} (°C)	ΔH_1 (J/g)	ΔH_2 (J/g)	E_a (kJ/mol)
5	257.91	291.10	-209.65	-411.97	93.90
10	273.91	304.99	-164.38	-402.96	
15	284.39	313.35	-139.71	-411.56	
20	291.37	321.05	-133.33	-410.15	

endothermic peaks at 225 and 240 °C might be, respectively, associated with a smectic–nematic transition and a nematic–isotropic transition. Similar results, the appearance of the enantiotropic mesophase transitions, have been obtained by other authors^{33–35} and were monitored by means of POM. For the two exothermic peaks, the first peak observed in the temperature range between 200 and 300 °C and the second was a considerably sharp peak at 300–310 °C. Here it should be pointed out that the two endothermic peaks related to the enantiotropic mesophase transitions accompanied the appearance of the first exothermic peak. Figure 8 illustrates that an exothermic trend became more distinct after 225 °C, indicating that a slow homopolymerization occurred before the appearance of the smectic mesophase and was accelerated after that. When the nematic mesophase was presented, the exothermic trend became more and more distinct. Accordingly, we consider that these LC mesophases may be performed jointly by a homopolymer and PBMB A, and the heat release may also be composed of contributions from the polymerization of amorphous domain and the LC mesophases. However, that may be difficult to distinguish.

The first exothermic peak can be associated with the PBMB A anionic homopolymerization. Based on the previous discussions in the mechanism of anionic polymerization, the anionic polymerization is related to the hydroxyl, whether the concentration of the hydroxyl groups, initially present in the epoxy prepolymer and those generated during the epoxy-amine polymerization, would affect the anionic polymerization process. A comparison of E_a values of the two anionic polymerization stages for PBMB A/MDA and PBMB A reveals that the occurrence of the PBMB A homopolymerization needs more energy, which may be ascribed to the discrepancy of the hydroxyl concentration. Because a substantial amount of hydroxyl groups is obtained from the PBMB A/MDA copolymerization, the hydroxyl concentration for PBMB A/MDA is higher than that for PBMB A. Accordingly, it is speculated that in the anionic polymerization stage of PBMB A/MDA, a substantial amount of hydroxyl groups obtained from the epoxy-amine polymerization stage makes it possible for more hydroxyl groups being protonated, which results in the increase of initiation of rate and polymerization reactivity.

For the second considerably sharp exothermic peak, it was referred to the thermal degradation reported by Lee.³⁵ However, we have held different views in this regard, since there is some doubt based on our DSC results. First, the observed heat of this stage was calculated as 181 kJ/mol (based on a molecular weight of 450 g/mol obtained by titration), implying that may not be simply due to the breaking of the covalent bond. The second, this peak, appearing in DSC with a considerably narrow temperature range, was not consistent with the peak of the thermal degradation. Last, the shift of DSC baseline after the exothermic peak

arising from the following three cases: weight loss, change in heating rate and change in heat capacity, did not appear. To resolve these doubts, the samples obtained respectively at 290 °C (PBMB A-1) and at 320 °C (PBMB A-2) were characterized by FT-IR spectra. Observed from the position of the C=N absorption band, it was found that the C=N stretching band appeared at 1623 cm⁻¹ for PBMB A-1 and at 1612 cm⁻¹ for PBMB A-2 (see Supporting Information). A combination of the calculated heat value with the enthalpy and the change of the CH=N absorption band at position show there are some interesting views as follows. First, the calculated heat value, being much lower than the energy of the covalent bond breakage, may result from the breaking of some noncovalent bonds, namely the deprotonation process of the Schiff-base moiety. It is, however, generally believed that the energy of the noncovalent bonds breakage is not up to our calculated heat value. But if we take into account the exothermic contribution of the homopolymerization, the higher calculated heat value should attribute to the two proportions' contribution. Second, the C=N stretching band arising from a slight shift to the lower wavenumber may be due to the occurrence of the deprotonation process of the Schiff-base moiety. Summarizing, the conjunct contribution of the coordination bond breakage and the heat release in the homopolymerization process may lead to the appearance of the sharp exothermic peak.

Schiff-Base Model Compound (SBM). Now that the anionic homopolymerization of the one-component LC diepoxide took place in the absence of tertiary amines, we wondered if the protonated Schiff-base moiety could also initiate the polymerization of the different types of epoxies. To this purpose, a Schiff-base model compound (SBM) was synthesized via the condensation of the aromatic aldehyde with the aromatic amine.

Figure 7 displays the thermogram of the neat diepoxides and the mixtures of diepoxides and SBM analyzed by nonisothermal DSC. The endothermic peaks appearing in the broad range 90–160 °C for the mixtures of diepoxides and SBM were due to SBM melting. It was noted that the nonisothermal polymerization curve for SBM/HWEP did exhibit an exothermic peak that failed to appear in those for SBM/DGEBA, SBM/BAEP, and the neat diepoxides. The appearance of this significant exothermic peak should be a strong hint for the polymerization heat release and indicated an occurrence of a polyetherification reaction. Although, the polyetherification reaction for epoxies is well described in the literature and can be thermally initiated and does not even require a specific initiator,^{38,50,51} it did not seem to support this view with the absence of the exothermic peak for the neat diepoxide. On the other hand, even if the reaction starts at about 180 °C, there is still a catalytic effect that should not be ignored. In our case, based on the initiation mechanism, it must be pointed out that the interactions between the Schiff-base moiety and the hydroxyl groups are essential for the initiation.

Regarding the effect of the concentration of the hydroxyl groups discussed above, HWEP, obviously possessing the higher hydroxyl concentration than DGEBA, may be easier to form the hydroxyl oxygen anion and then initiate the anionic polymerization. Meanwhile, it should be noted that PBMB A, possessing the lower hydroxyl concentration than HWEP, could be involved in the homopolymerization. This contrary situation should be related with the occurrence of the enantiotropic mesophases, because the unexpected homopolymerization of PBMB A took place accompanying the appearance of the enantiotropic mesophase transitions. Owing to the formation of these mesophases, the highly π -conjugated Schiff-base moiety contributes to the

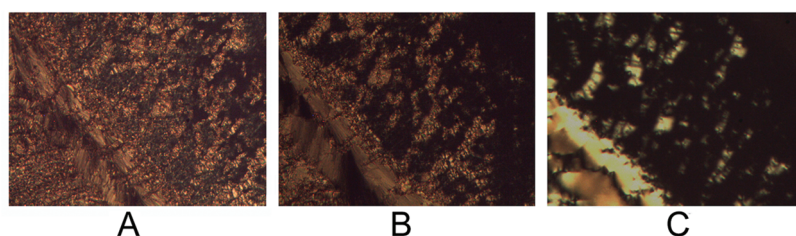


Figure 9. Smectic morphologies observed at 225 °C (A) and stabilized at 210 °C for 30 min (B) and for 120 min (C) by POM. Magnification: 200× .

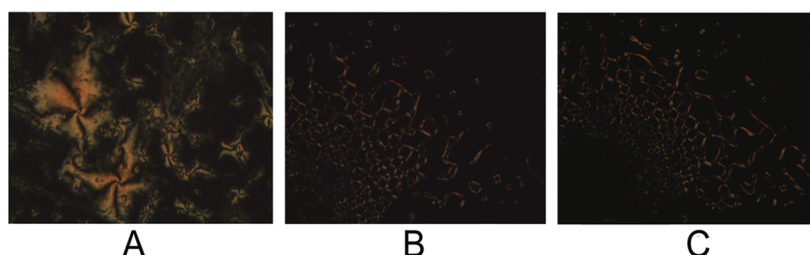


Figure 10. Nematic morphologies observed at 240 °C (A) and stabilized at 210 °C for 30 min (B) and for 50 min (C) by POM. Magnification: 200× .

π - π stacking that may enhance the initiation ability of the mesogenic unit. Accordingly, to explain the specific role of the highly conjugated Schiff-base moiety in polymerization of the epoxies, an electronic sink effect should be proposed. Based on Drude's free electron theory,⁵² it is a simplified model of electrical conduction and can be represented as a process of accumulation of free electrons inside a battery-positive. Due to the molecular electronic resonance formed by the $D \cdots [H^+] \cdots A$ assembly, the electron sink effect may be produced.^{53–55} Accordingly, the protonated Schiff-base moiety resulting from the $D \cdots [H^+] \cdots A$ assembly might serve as an electronic sink for imine/amine or imine/hydroxy chemistry (see Figures 4 and 5). It is just because of the electronic sink effect that the mobility of the amino is decreased, which leads to the increase of the E_a value for the epoxy-amine polymerization. It is also due to the presence of the electronic sink effect that the alkoxy anions can be formed in the "protonation-induced" assembly process, thus, resulting in the occurrence of the unexpected anionic polymerization.

Stabilization of Mesophases. Depending on annealing temperature, two types of ordered structure, the smectic phase and the nematic phase, were observed under POM, as shown in Figures 9A and 10A. The smectic phase and the nematic phase formed in the temperature range of 218–232 °C and 232–245 °C, respectively, and the onset polymerization temperature of PB MBA was about 200 °C, which means that the ordered structures may be stabilized directly by the polymer network. Inspection by POM showed that, at 210 °C, the smectic phase gradually disappeared and became discontinuous with the increase of the polymerization time (see Figure 9B,C). The similar results were obtained when the sample possessing the nematic phase was heated at 210 °C for different time (see Figure 10B,C). Additionally, the fixed domain of the smectic phase and the nematic phase could be maintained for at least 3 h and for no more than 50 min, after then they were transformed into an isotropic phase. To confirm the ordered structures presenting in the polymer network, the crystalline morphology was examined using WAXD. The room temperature WAXD

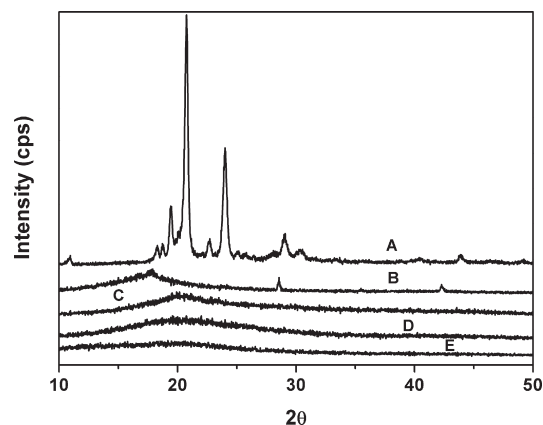


Figure 11. Room temperature WAXD patterns for PB MBA (A), S30 (B), S120 (C), N30 (D), and N50 (E).

patterns of PB MBA, S30, S120, N30, and N50 are presented in Figure 11. PB MBA displayed a typical WAXD pattern of a liquid crystal. After the isothermal treatment, WAXD patterns of S30, S120, N30, and N50 clearly showed that, although the amorphous structure appeared, the diffraction peak of the crystal structures did not entirely disappear.

During the isothermal treatment, the mesophase was stabilized after that partially disappeared. This may be due to the partial diepoxide compounds were involved in the PB MBA homopolymerization that increased the length of the molecule chain and broke the ordered aggregation of the mesogens. Owing to the lower polymerization temperature, the diffusion ability of the rest of the aggregative diepoxide compounds was restricted by long-chain macromolecules to some degree. Therefore, the partial PB MBA involved in the homopolymerization that formed the isotropic phase and the partial PB MBA possessing the mesophase became immobile and was stabilized. It can also be used to explain the appearance of the amorphous structure and the disappearance of the crystal structure confirmed by WAXD. With the increase of isothermal treatment time, the mobility of

the long-chain macromolecules is increased, which may release the restricted LC monomers to react. The formed LC polymer may be identified as a side-chain LC polymer that can form LC mesophases.^{56,57} Therefore, the stabilization mesophases may be attributed to either the monomer or the polymer, but that may be difficult to distinguish. Furthermore, the difference in the holding periods between the stabilization smectic phase and nematic phase may be related to the structural characteristics of them. It is well-known that there are two fundamental orders, orientational order and translational order. For a crystal, 3-dimensional periodic array of atoms or molecules are orientational and translational order. For the LC mesophase, with the increase of temperature, the orientational order will be lost first, but the translational order will be retained. For the nematic phase, however, it is the only mesophase without the translational order at higher temperature.⁵⁸ Thereby, the stabilized nematic phase exhibited the shorter holding period than the stabilized smectic phase. Altogether, we can state that these ordered structures can be stabilized by the anionic homopolymerization depending on the polymerization time and temperature. It is conceivable, even, that this kind of method opens new strategies for the design of materials with well-dispersed LC mesophases. However, the work, how to control the dispersion homogeneity, and the size of the discontinuous phase domain, is important and will be further studied as our next work.

CONCLUSIONS

Based on the structure–property relationship, the study of the highly π -conjugated Schiff-base moiety in polymerization of PBMBA has been implemented. In the case of PBMBA/MDA copolymerization, the DSC curve showed two exotherms, being the first attributed to the copolymerization of the epoxy and MDA, and the second attributed to the anionic homopolymerization of the epoxide. With the rigid C=N groups and the benzene rings at alternate positions in the main chain acting as the proton acceptor and the amino or hydroxyl proton in the polymerization system acting as the proton donor, the $D \cdots [H^+] \cdots A$ assembly forms. The evidence in the FT-IR spectrum and the UV–vis absorbance spectrum show that the shift transitions of the characteristic peak for the C=N stretching deformations are consistent with the assembly behavior of $D \cdots [H^+] \cdots A$ between the Schiff-base moiety and the amino group.

Due to the molecular electronic resonance formed by the $D \cdots [H^+] \cdots A$ assembly, during the copolymerization process, the protonated Schiff-base moiety serving as the electronic sink can not only hinder the mobility of the amino groups, leading to the increase of the epoxy-amine polymerization E_a , but also capture the hydroxyl groups initially present in the epoxy prepolymer and those generated during the epoxy-amine copolymerization, leading to the formation of alkoxy anions. The formed key intermediate alkoxy anions reacting with another hydroxyl groups through the ionic transition effect results in the formation of hydroxyl oxygen anions, which is considered to be the initiation process of the anionic polymerization. This initiation mechanism of the anionic polymerization proposed first by us is also suitable for the anionic homopolymerization of the one-component LC diepoxide and the preparative SBM initiating the high hydroxyl concentration epoxy anionic polymerization. Furthermore, using this mechanism of the anionic polymerization, the smectic and nematic phases presenting in the anionic

homopolymerization reaction were well stabilized. This kind of method, via the chemical process to obtain the LC mesophases based on the structure–property relationship, opens new strategies for the design of the PDLCs materials.

ASSOCIATED CONTENT

S Supporting Information. Figure showing FT-IR spectra of PBMBA-1 and PBMBA-2. This material is available free of charge via the Internet at <http://pubs.acs.org>.

AUTHOR INFORMATION

Corresponding Author

*Tel.: +86 20 85232302. Fax: +86 20 85231058. E-mail: xk@gic.ac.cn.

REFERENCES

- (1) Pascault, J. P.; Williams, R. J. J. *Epoxy Polymers: New Materials and Innovations*; Wiley-VCH: Germany, 2010.
- (2) Uddin, M. A.; Chan, H. P.; Chow, C. K. *Chem. Mater.* **2004**, *16*, 4806–4811.
- (3) Bekyarova, E.; Thostenson, E. T.; Yu, A.; Kim, H.; Gao, J.; Tang, J.; Hahn, H. T.; Chou, T.-W.; Itkis, M. E.; Haddon, R. C. *Langmuir* **2007**, *23*, 3970–3974.
- (4) Cao, Q.; Xia, M. G.; Shim, M.; Rogers, J. A. *Adv. Funct. Mater.* **2006**, *16*, 2355–2362.
- (5) Meng, L. M.; Yuan, Y. C.; Rong, M. Z.; Zhang, M. Q. *J. Mater. Chem.* **2010**, *20*, 6030–6038.
- (6) Jones, A. S.; Rule, J. D.; Moore, J. S.; White, S. R.; Sottos, N. R. *Chem. Mater.* **2006**, *18*, 1312–1317.
- (7) Altebaeumer, T.; Gotsmann, B.; Pozidis, H.; Knoll, A.; Duerig, U. *Nano Lett.* **2008**, *8*, 4398–4403.
- (8) Motoyuki, I.; Murino, K.; Miwa, Y.; Yasuhiro, O.; Hidehiro, K. *J. Am. Chem. Soc.* **2009**, *131*, 16342–16343.
- (9) Choi, S.; Coronas, J.; Jordan, E.; Oh, W.; Nair, S.; Onorato, F.; Shantz, D. F.; Tsapatsis, M. *Angew. Chem., Int. Ed.* **2008**, *47*, 552–555.
- (10) Wu, C. C.; Hsu, S. L.-C. *J. Phys. Chem. C* **2010**, *114*, 2179–2183.
- (11) Tercjak, A.; Serrano, E.; Garcia, I.; Mondragon, I. *Acta Mater.* **2008**, *56*, 5112–5122.
- (12) Tang, L. M.; Whalen, J.; Schutte, G.; Weder, C. *ACS Appl. Mater. Interfaces* **2009**, *1*, 688–696.
- (13) Zou, J. H.; Liu, L. W.; Chen, H.; Khondaker, S. I.; McCullough, R. D.; Huo, Q.; Zhai, L. *Adv. Mater.* **2008**, *20*, 2055–2060.
- (14) Burke, C. P.; Shi, Y. *Angew. Chem., Int. Ed.* **2006**, *45*, 4475–4478.
- (15) Elemans, J. A. A. W.; Van-Hameren, R.; Nolte, R. J. M.; Rowan, A. E. *Adv. Mater.* **2006**, *18*, 1251–1266.
- (16) Diegelmann, S. R.; Gorham, J. M.; Tovar, J. D. *J. Am. Chem. Soc.* **2008**, *130*, 13840–13841.
- (17) Hoeben, F. J. M.; Jonkheijm, P.; Meijer, E. W.; Schenning, A. P. H. J. *Chem. Rev.* **2005**, *105*, 1491–1546.
- (18) Chen, X. F.; Shen, Z. H.; Wan, X. H.; Fan, X. H.; Chen, E. Q.; Ma, Y. G.; Zhou, Q. F. *Chem. Soc. Rev.* **2010**, *39*, 3072–3101.
- (19) Goel, M.; Jayakannan, M. *J. Phys. Chem. B* **2010**, *114*, 12508–12519.
- (20) Kim, F. S.; Ren, G. Q.; Jenekhe, S. A. *Chem. Mater.* **2011**, *23*, 682–732.
- (21) Samitsu, S.; Takanishi, Y.; Yamamoto, J. *Macromolecules* **2009**, *42*, 4366–4368.
- (22) Sinnokrot, M. O.; Sherrill, C. D. *J. Am. Chem. Soc.* **2004**, *126*, 7690–7697.
- (23) Roy, D.; Cambre, J. N.; Sumerlin, B. S. *Prog. Polym. Sci.* **2010**, *35*, 278–301.
- (24) Hameed, N.; Guo, Q. P.; Xu, Z. G.; Hanley, T. L.; Mai, Y. W. *Soft Matter* **2010**, *6*, 6119–6129.

- (25) Hu, D.; Xu, Z. G.; Zeng, K.; Zheng, S. X. *Macromolecules* **2010**, *43*, 2960–2969.
- (26) Grinberg, S.; Linder, C.; Kolot, V.; Waner, T.; Wiesman, Z.; Shaubi, E.; Heldman, E. *Langmuir* **2005**, *21*, 7638–7645.
- (27) Zhu, Y. C.; Wang, B.; Gong, W.; Kong, L. M.; Jia, Q. M. *Macromolecules* **2006**, *39*, 9441–9445.
- (28) Hoppe, C. E.; Galante, M. J.; Oyanguren, P. A.; Williams, R. J. J. *Macromolecules* **2002**, *35*, 6324–6331.
- (29) Hoppe, C. E.; Galante, M. J.; Oyanguren, P. A.; Williams, R. J. J. *Macromolecules* **2004**, *37*, 5352–5357.
- (30) Maschke, U.; Coqueret, X.; Benmouna, M. *Macromol. Rapid Commun.* **2002**, *23*, 159–170.
- (31) Sannier, L.; Siddiqi, H. M.; Maschke, U.; Dumon, M. *J. Appl. Polym. Sci.* **2004**, *92*, 2621–2628.
- (32) Higgins, D. A. *Adv. Mater.* **2000**, *12*, 251–264.
- (33) Ochi, M.; Takashima, H. *Polymer* **2001**, *42*, 2379–2385.
- (34) Mormann, W.; Bröcher, M. *Polymer* **1999**, *40*, 193–198.
- (35) Lee, J. Y.; Song, Y. W.; Shim, M. J. *J. Ind. Eng. Chem.* **2004**, *10*, 601–607.
- (36) Doyle, L. D. *Nature (London)* **1965**, *207*, 290–291.
- (37) Wise, C. W.; Cook, W. D.; Goodwin, A. A. *Polymer* **1997**, *38*, 3251–3261.
- (38) Mijovic, J.; Wijaya, J. *Macromolecules* **1994**, *27*, 7589–7600.
- (39) Zhang, Y. X.; Vyazovkin, S. *J. Phys. Chem. B* **2007**, *111*, 7098–7104.
- (40) Vyazovkin, S. *Macromolecules* **1996**, *29*, 1867–1873.
- (41) Deng, Y.; Martin, C. *Macromolecules* **1994**, *27*, 5141–5146.
- (42) Buist, G. J.; Barton, J. M.; Howlin, B. J.; Jones, J. R.; Parker, M. J. *J. Mater. Chem.* **1996**, *6*, 911–915.
- (43) Sek, D.; Iwan, A.; Jarzabek, B.; Kaczmarczyk, B.; Kasperczyk, J.; Mazurak, Z.; Domanski, M.; Karon, K.; Lapkowski, M. *Macromolecules* **2008**, *41*, 6653–6663.
- (44) Rosenthal, J.; Hodgkiss, J. M.; Young, E. R.; Nocera, D. G. *J. Am. Chem. Soc.* **2006**, *128*, 10474–10483.
- (45) Ward, B.; Chang, C. K.; Young, R. J. *Am. Chem. Soc.* **1984**, *106*, 3943–3950.
- (46) Rozenberg, B. A. *Adv. Polym. Sci.* **1986**, *75*, 113–165.
- (47) Heise, M. S.; Martin, G. C. *Macromolecules* **1989**, *22*, 99–104.
- (48) Fernández-Francos, X.; Cook, W. D.; Serra, A.; Ramis, X.; Liang, G. G.; Salla, J. M. *Polymer* **2010**, *51*, 26–34.
- (49) Rebizant, V.; Abetz, V.; Tournilhac, F.; Court, F.; Leibler, L. *Macromolecules* **2003**, *36*, 9889–9896.
- (50) Rokicki, G. *Prog. Polym. Sci.* **2000**, *25*, 259–342.
- (51) Girard-Reydet, E.; Riccardi, C. C.; Sautereau, H.; Pascault, J. P. *Macromolecules* **1995**, *28*, 7599–7607.
- (52) Drude, P. *Ann. Phys. (Berlin)* **1900**, *306*, 566–613.
- (53) Nash, H. M.; Lu, R. Z.; Lane, W. S.; Verdine, G. L. *Chem. Biol.* **1997**, *4*, 693–702.
- (54) Turbeville, T. D.; Zhang, J. S.; Hunter, G. A.; Ferreira, G. C. *Biochemistry* **2007**, *46*, 5972–5981.
- (55) Diaz, E.; Anton, D. L. *Biochemistry* **1991**, *30*, 4078–4081.
- (56) Callau, L.; Giamberini, M.; Reina, J. A.; Mantecon, A. J. *Polym. Sci., Polym. Chem.* **2006**, *44*, 1877–1889.
- (57) Akiyama, E.; Nagase, Y.; Koide, N. *Makromol. Chem., Rapid Commun.* **1993**, *14*, 251–259.
- (58) Holmes, M. C.; Charvolin, J. *J. Phys. Chem.* **1984**, *88*, 810–818.